Available online at www.sciencedirect.com
ScienceDirect
Journal of Power Sources 168 (2007) 501–508
JOURNAL OF POWER SOURCES
www.elsevier.com/locate/jpowsour

Electrochemical performance and kinetics of $Li_{1+x}(Co_{1/3}Ni_{1/3}Mn_{1/3})_{1-x}O_2$ cathodes and graphite anodes in low-temperature electrolytes

M.C. Smart [a], J.F. Whitacre [a], B.V. Ratnakumar [a,*], K. Amine [b]

[a] *Jet Propulsion Laboratory, California Institute of Technology, M/S: 277-207, 4800 Oak Grove Drive, Pasadena, CA 91109, United States*
[b] *Argonne National Laboratory, 9700 South Cass Avenue, Bldg. 205 Argonne, IL 60439, United States*

Received 26 September 2006; accepted 9 October 2006
Available online 12 March 2007

Abstract

Lithium-ion batteries have started replacing the conventional aqueous nickel-based battery systems in space applications, such as planetary landers, rovers, orbiters and satellites. The reasons for such widespread use of these batteries are the savings in mass and volume of the power subsystems, resulting from their high gravimetric and volumetric energy densities, and their ability to operate at extreme temperatures. In our pursuit to further enhance the specific energy as well as low-temperature performance of Li-ion batteries, we have been investigating various layered lithiated metal oxides, e.g., $LiCoO_2$, $LiNi_{0.8}Co_{0.2}$ and $LiNi_{0.8}Co_{0.15}Al_{0.05}O_2$, as well as different low-temperature electrolytes, including ternary and quaternary carbonate mixtures with various co-solvents. In this paper, we report our recent studies on $Li_{1+x}(Co_{1/3}Ni_{1/3}Mn_{1/3})_{1-x}O_2$ cathodes, combined with three different low-temperature electrolytes, i.e.: (1) 1.0 M $LiPF_6$ in EC:EMC (20:80), (2) 1.2 M $LiPF_6$ in EC:EMC (20:80) and (3) 1.2 M $LiPF_6$ in EC:EMC (30:70). Electrical performance characteristics were determined in laboratory glass cells at different discharge rates and different temperatures. Further, individual electrode kinetics of both $Li_{1+x}(Co_{1/3}Ni_{1/3}Mn_{1/3})_{1-x}O_2$ cathodes and MCMB graphite anodes were determined at different temperatures, using dc micropolarization, Tafel polarization and electrochemical impedance spectroscopy (EIS). Analysis of these data has led to interesting trends relative to the effects of solvent composition and salt concentration, on the electrical performance and on the kinetics of cathode and anode. Published by Elsevier B.V.

Keywords: Lithium-ion cells; Low-temperature electrolytes; Performance; Kinetics

1. Introduction

Lithium-ion batteries are preferred to the conventional aqueous nickel rechargeable battery systems in several space applications, such as planetary landers [1], rovers [2], orbiters and satellites. The reasons for such widespread use of Li-ion batteries are the benefits in mass and volume, both of which are always critical in any mission, resulting from a three-fold enhancement in the specific energy and about a six-fold benefit in the energy density. In addition, the ability to operate at extreme temperatures greatly simplifies their thermal management. A combination of these desirable attributes of lithium-ion batteries will result in significant enhancement of space missions, or can even be mission enabling in some cases, e.g., the on-going Mars Exploration Rovers.

In order to address the challenges of future missions to 'Moon, Mars and Beyond' as envisaged by NASA's Exploration Systems Mission Directorate (ESMD), we undertook a technology development endeavor to further enhance the specific energy and low-temperature performance of Li-ion batteries. In this pursuit, we have been examining various layered lithiated metal oxides as well as different low-temperature electrolytes [3,4]. Compared to the conventional $LiCoO_2$, $LiNi_{0.8}Co_{0.2}$ and $LiNi_{0.8}Co_{0.15}Al_{0.05}O_2$ cathodes, $LiCo_{1/3}Ni_{1/3}Mn_{1/3}O_2$ (termed as NMC) cathodes provide higher specific capacity and also enhanced thermal stability. Accordingly, this material is being studied in detail by several research groups, for a range of applications [5–10]. It would be interesting to verify the performance of such cathodes in conjunction with low-temperature electrolytes, and to determine the performance limiting aspects at low-temperature. Given that the rate capability of $LiCo_{1/3}Ni_{1/3}Mn_{1/3}O_2$ cathodes has been reported to be poorer than that of $LiCoO_2$ cathodes [6,7,10] there is particular interest in determining if the low-temperature capability of

* Corresponding author. Tel.: +1 818 354 0110; fax: +1 818 393 6951.
E-mail address: ratnakumar.v.bugga@jpl.nasa.gov (B.V. Ratnakumar).

0378-7753/$ – see front matter. Published by Elsevier B.V.
doi:10.1016/j.jpowsour.2006.10.106

the material is adversely affected by limited lithium diffusivity. Choi and Manthiram [10] have reported that over 80% of the capacity is maintained at 2 C rates compared to the capacity delivered at C/10, however, the rate capability as a function of temperature and as function of electrolyte type was not investigated.

In this paper, we studied the electrochemical performance of $Li_{1+x}(Co_{1/3}Ni_{1/3}Mn_{1/3})_{1-x}O_2$, provided by Argonne National Laboratory, in three different low-temperature electrolytes: (1) 1.0 M $LiPF_6$ in EC (ethylene carbonate):EMC (ethyl methyl carbonate) (20:80, v/v%), (2) 1.2 M $LiPF_6$ in EC:EMC (20:80, v/v%) and (3) 1.2 M $LiPF_6$ in EC:EMC (30:70, v/v%), at different discharge rates and temperatures. Even though electrolytes with quaternary solvent mixtures and with ester co-solvents showed impressive low-temperature performance as reported in our earlier publications, the selected electrolytes are also expected to perform well. Besides, the third electrolyte solution is being examined by DoE for hybrid car applications. In addition to the performance at various temperatures, the electrochemical kinetics of the $LiCo_{1/3}Ni_{1/3}Mn_{1/3}O_2$ cathodes as well as the graphitic anodes were determined from dc micropolarization, Tafel and electrochemical impedance spectroscopy (EIS) at various temperatures. Interesting trends have been observed both in terms of the performance and the electrode kinetics at different temperature, as a function of the ratio of EC and EMC and the concentration of the electrolyte salt.

2. Experimental

The cathode and anode materials for these studies contained $Li_{1+x}(Co_{1/3}Ni_{1/3}Mn_{1/3})_{1-x}O_2$ ($x = 0.1$) from Seimi, Japan and MCMB-10-28 graphite from Osaka Gas. The cathodes, coated on Al foil, contained 84% of active material, 8% of conductive diluent and 8% of binder. The anode, on the other hand, had the composition of 90% of active material, 2% of vapor grown carbon fiber (VGCF) as conductive diluent and 8% binder. The electrodes thus supplied by Argonne National Laboratory were trimmed to the size (~6.5″ × 1.5″), bagged with polyethylene separators, and rolled into a jelly roll using Teflon mandrills, which were later inserted into glass cells sealed with O-ring seals. The electrode jelly rolls also had reference electrodes in the form of lithium cold-welded onto Ni foils. The stock solutions for the electrolytes were obtained from EM Sciences, Inc. All the cell fabrication operations were performed in a dry room with less than 1% humidity, while the electrolyte filling or activation was performed in an argon-filled glove box. All the electrochemical performance studies, such as charging, discharging and cycling at different temperatures were carried out using an Arbin battery system and Tenney Jr environmental chambers. For basic electrochemical studies, a combination of an EG&G 273A potentiostat and an EG&G Frequency Response Analyzer was used with the support of a Softcorr program for the dc polarization measurements and a M382 program was used for the electrochemical impedance spectroscopy (EIS) measurements. All measurements were performed at 25 ± 2 °C, unless mentioned otherwise.

3. Results and discussions

As mentioned above, the electrochemical performance was determined in the three different electrolytes at various rates of charge and discharge and at different temperatures. To further understand the observed trends in the performance, electrochemical kinetics for both anode and cathode were determined, using dc Tafel and dc micropolarization as well as electrochemical impedance spectroscopy.

3.1. Electrochemical performance

The typical charge–discharge characteristics of one of the three cells during the formation process are illustrated in Fig. 1, in which the cell voltage, anode potential and cathode potential are displayed. As may be seen from this figure, the cell is well balanced, i.e., the cathode and anode capacities are well matched with the selected areas and active material loadings. At the end of charge, the anode potentials remained positive to Li, thus ensuring that there is some buffer in the anode capacity and that there would not be any lithium plating under normal conditions. Table 1 shows further details on the charge and discharge capacities and coulombic efficiency in the first five formation cycles. As may be seen from the figure, all these characteristics are nearly identical for the electrolytes studied here.

Relative to the rate capability at room temperatures, the electrolyte with low salt concentration and low EC-content yielded ~89% of the low rate (0.2 C) capacity at 0.8 C, while the electrolyte with higher salt and low EC gave a capacity of 90.5% and the cell with high salt and high EC gave ~93%. Thus, it is clear that high EC formulations, and electrolytes with high salt concentrations, perform better at high discharge rates at ambient temperatures.

Fig. 2 illustrates the performance of these cells at low temperatures, specifically at −40 °C and −50 °C. The percent capacities under these conditions are also listed in Table 2. As may be seen from the figure, at −40 °C using a low discharge rate of C/20, the performance is the best with the electrolyte with high EC-content, while the low EC solution, especially with

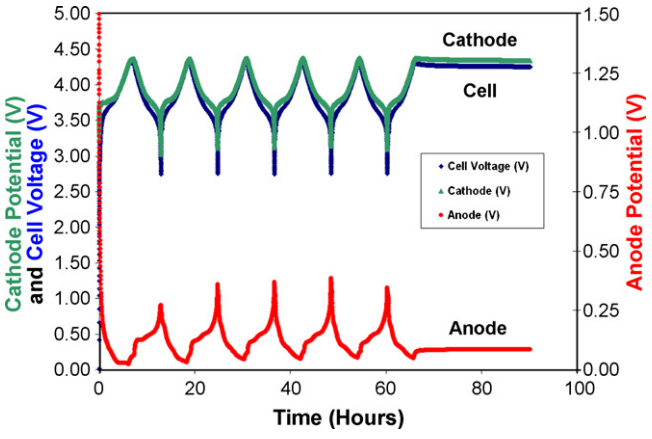

Fig. 1. Charge–discharge curves of $LiNi_{1/3}Mn_{1/3}Co_{1/3}O_2$-C laboratory test cell with 1.0 M $LiPF_6$/EC:EMC (20:80) electrolyte solution during the formation cycles. Also shown are the individual potentials of cathode and anode.

Table 1
Formation characteristics of graphite-$LiNi_{1/3}Co_{1/3}Mn_{1/3}O_2$ cells in (a) 1.0 M $LiPF_6$/EC:EMC (20:80), (b) 1.2 M $LiPF_6$/EC:EMC (20:80) and (c) 1.2 M $LiPF_6$/EC:EMC (30:70) electrolyte solutions

Electrolyte type	Charge capacity (mAh) 1st cycle	Discharge capacity (mAh) 1st cycle	Irreverisible capacity (1st cycle) (mAh)	Couloumbic efficiency (1st cycle) (%)	Charge capacity (mAh) 5th cycle	Reversible capacity (mAh) 5th cycle	Cumulative irreversible capacity (1st–5th cycle) (mAh)	Coulombic efficiency (5th cycle) (%)
1.0 M $LiPF_6$ EC + EMC (20:80, v/v%)	164.9	134.1	30.8	81.3	139.2	135.8	40.7	97.6
1.2 M $LiPF_6$ EC + EMC (20:80, v/v%)	168.5	140.6	27.9	83.4	142.0	139.1	35.2	98.0
1.2 M $LiPF_6$ EC + EMC (30:70, v/v%)	156.0	127.9	28.1	82.0	129.1	126.5	39.7	98.0

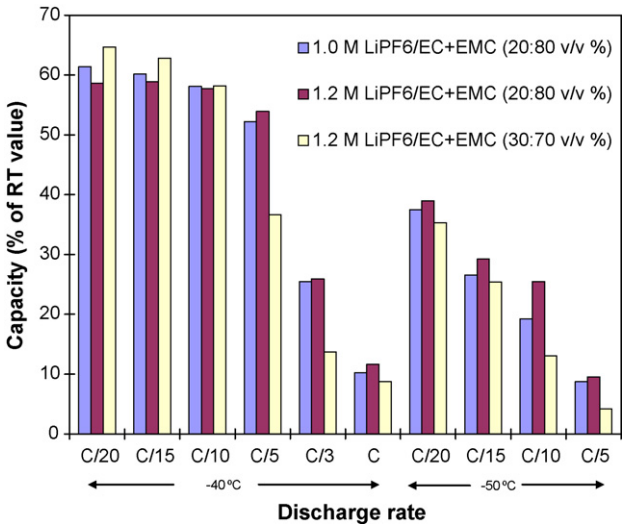

Fig. 2. Discharge capacities of $LiNi_{1/3}Mn_{1/3}Co_{1/3}O_2$-C laboratory test cells with (1) 1.0 M $LiPF_6$/EC:EMC (20:80), (2) 1.2 M $LiPF_6$/EC:EMC (20:80) and (3) 1.2 M $LiPF_6PF_6$/EC:EMC (30:70) electrolyte solutions at different discharge rates and temperatures.

low salt concentration gave the poorest performance. At high discharge rates, however, the trend is reversed. At a discharge rate exceeding C/5, the low EC solutions far outperformed the high EC-content solution, with the high salt concentration, helping even more. A similar trend is also observed in the discharge capacities at −50 °C; the benefits of low EC proportions are evident even at low discharge rates, i.e., C/10–C/5. These trends are better illustrated in Fig. 3A and B, which show the discharge curves at −40 °C at C/15 and C/5, respectively. At C/5, the discharge voltages as well as discharge capacity are considerably diminished in high EC-content electrolyte. The improved low-temperature performance in electrolytes with low EC-content, especially at high rates, may be attributed to their lower viscosity and higher ionic conductivity. The enhanced performance delivered with the use of electrolytes containing higher salt concentration may be understood in terms of reduced mass transfer polarization, especially at high discharge rates. Though lower salt concentrations are preferred for lowering the viscosity and thus improving the ionic conductivity [11] and performance characteristics, it appears that at high discharge rates, the availability of adequate lithium ions at the interface is critical, especially at high discharge rates and low temperatures.

3.1.1. Electrochemical kinetics

Even though the performance in the three electrolytes is nearly identical at ambient temperature, there are some differences at low temperatures, especially being evident at low and high discharge rates. In order to gain further understanding into these performance variations, electrochemical kinetics were determined using dc polarization methods as well as electrochemical impedance spectroscopy (EIS).

3.1.2. Electrochemical impedance spectroscopy (EIS)

Electrochemical impedance spectroscopy measurements were made on the three cells at different temperatures, i.e.,

Table 2
Summary of performance characteristics graphite–$LiNi_{1/3}Co_{1/3}Mn_{1/3}O_2$ cells in (a) 1.0 M $LiPF_6$/EC:EMC (20:80), (b) 1.2 M $LiPF_6$/EC:EMC (20:80) and (c) 1.2 M $LiPF_6$/EC:EMC (30:70) electrolyte solutions at different discharge rates and temperatures

Temperature (°C)	Current (mA)	Rate	1.0 M $LiPF_6$ in EC + EMC (20:80, v/v%)		1.2 M $LiPF_6$ in EC + EMC (20:80, v/v%)		1.2 M $LiPF_6$ in EC + EMC (30:70, v/v%)	
			Capacity (mAh)	Percent (%)	Capacity (mAh)	Percent (%)	Capacity (mAh)	Percent (%)
23	25.00	C/5	135.8	100.0	139.1	100.0	126.5	100.0
−40	6.25	C/20	83.4	61.4	81.6	58.7	81.8	64.7
	8.33	C/15	81.7	60.2	81.9	58.9	79.5	62.8
	12.50	C/10	78.9	58.1	80.3	57.7	73.6	58.2
	25.00	C/5	70.9	52.2	75.0	53.9	46.4	36.6
	41.67	C/3	34.6	25.5	36.1	25.9	17.3	13.7
	62.50	C	13.9	10.3	16.2	11.6	11.1	8.8
−50	6.25	C/20	50.9	37.5	54.2	39.0	44.7	35.3
	8.33	C/15	36.0	26.5	40.6	29.2	32.2	25.4
	12.50	C/10	26.1	19.2	35.5	25.5	16.5	13.1
	25.00	C/5	11.9	8.7	13.3	9.5	5.3	4.2

at 25 °C, 0 °C, −20 °C, −30 °C and −40 °C. These measurements were all made in a fully charged state, i.e., 100% state of charge (corresponding to the cell being charged to 4.30 V) over a wide frequency range of 10^5 Hz to 10^{-2} Hz. Fig. 4 shows the typical Nyquist EIS plot of the cathode, anode and the cell at −30 °C. As may be seen from the figure, the anode seems to be contributing more to the overall cell impedance. This is consistent with what we have seen in past with other electrode systems, where the anode kinetics tend to be faster than at the cathode at room temperature and at temperatures below −20 °C, the SEI on the surface of the anode typically contributes a significant portion towards the overall cell impedance. Figs. 5 and 6 show the EIS behavior of the cathode and anode, respectively, at different temperatures in the three different electrolytes. Even though the impedance plots of the cathode look fairly similar, there are some differences. The series impedance and the overall impedance seem to be slightly lower for the high-EC solution at ambient temperatures, while the trend is reversed at low temperatures. The anode EIS plots (Fig. 6), on the other hand, are much more similar in the three electrolytes; at least as a function of temperature. A more detailed analysis of the EIS data, with suitable equivalent circuits and a quantitative interpretation in terms of the changes in the kinetic parameters will be provided in our future publication. For a semi-quantitative understanding

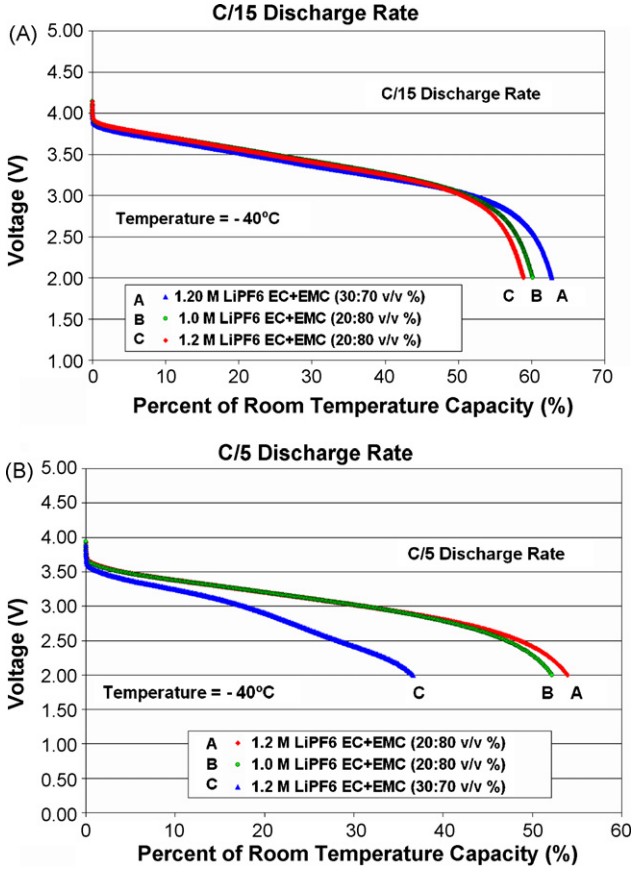

Fig. 3. Performance characteristics of $LiNi_{1/3}Mn_{1/3}Co_{1/3}O_2$-C laboratory test cell in (1) 1.0 M $LiPF_6$/EC:EMC (20:80), (2) 1.2 M $LiPF_6$/EC:EMC (20:80) and (3) 1.2 M $LiPF_6$/EC:EMC (30:70), electrolyte solutions at −40 °C and at (A) C/15 and (B) C/5 rates.

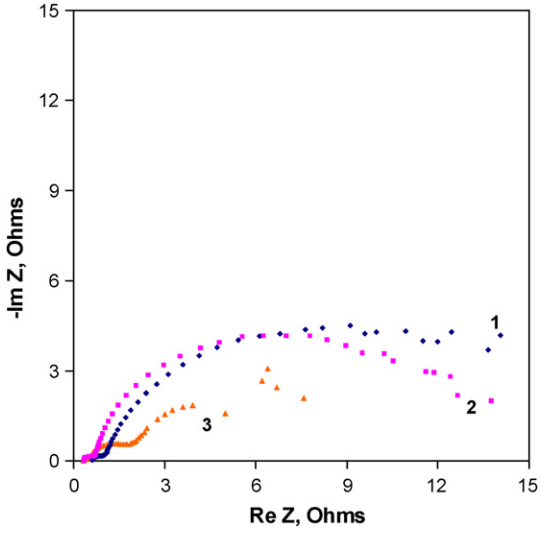

Fig. 4. EIS plots of (1) $LiNi_{1/3}Mn_{1/3}Co_{1/3}O_2$-C laboratory test cell with 1.0 M $LiPF_6$/EC:EMC (20:80) solution at −30 °C. Plots 2 and 3 correspond to the anode and cathode behavior.

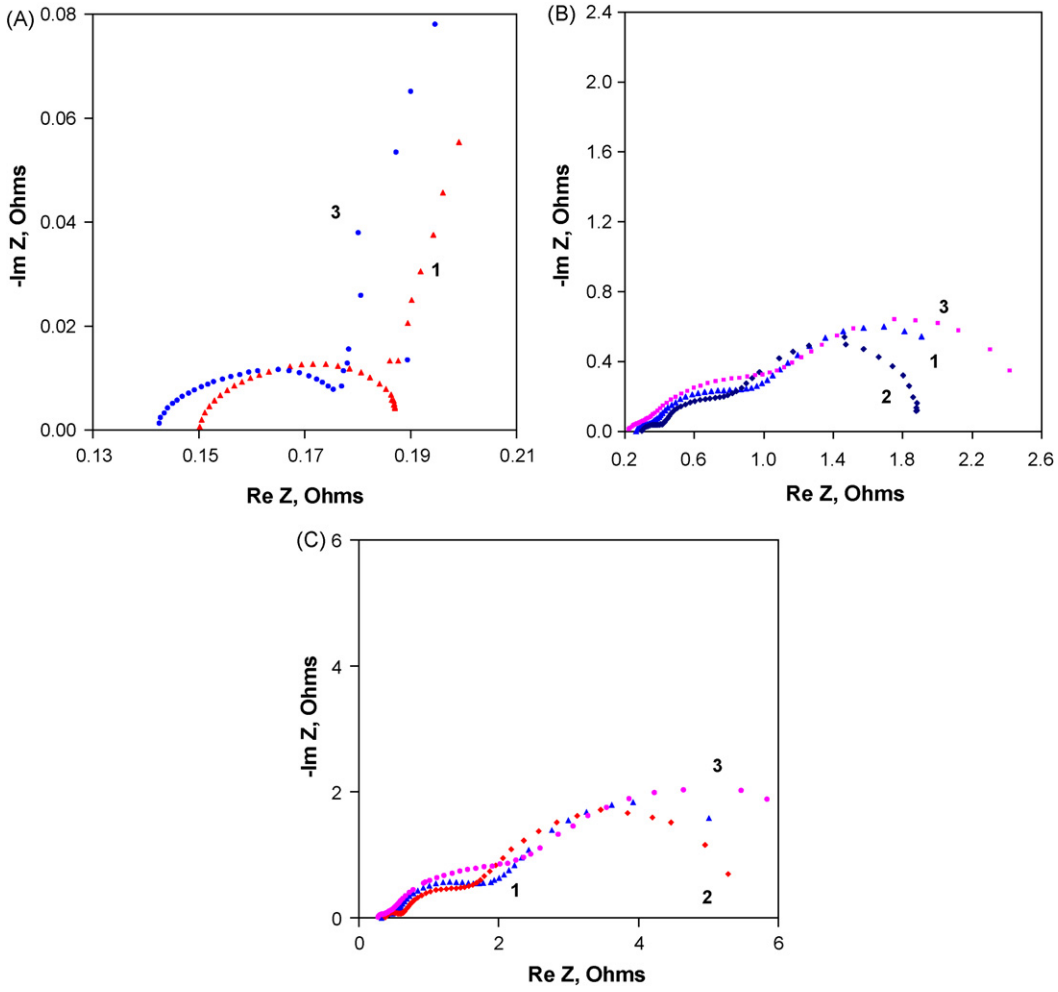

Fig. 5. EIS plots of $LiNi_{1/3}Mn_{1/3}Co_{1/3}O_2$ cathode in (1) 1.0 M $LiPF_6$/EC:EMC (20:80), (2) 1.2 M $LiPF_6$/EC:EMC (20:80) and (3) 1.2 M $LiPF_6$/EC:EMC (30:70) electrolyte solutions at (A) 25 °C, (B) −20 °C and (3) −30 °C, respectively.

of the impedance values as a function of the electrolyte composition, the cathode impedance at three different frequencies, for example, at 200 Hz, 1 Hz and 0.05 Hz, are plotted as a function of temperature in Fig. 7. The reason for choosing these three frequencies is due to the fact that they lie in the ranges corresponding to the SEI charging, charge transfer kinetics and diffusional impedance, respectively. As may be seen from the figure, the impedance values increase sharply at low temperatures, more significantly at low frequencies. This increase is also more noticeable with the electrolyte containing high EC, compared to the low-EC formulations. Furthermore, the impedance at any temperature and frequency is lower for the solution containing low-EC as well as low salt concentration.

3.1.3. dc linear polarization

To augment the EIS measurements, dc polarization measurements were made at low polarization (±5 mV), which permits linearization of the electrochemical rate equation and thus simplifies the determination of polarization resistance or exchange current density. For example, Fig. 8 shows such linear polarization plots of the carbon anodes in 1.0 M $LiPF_6$/20:80 EC:EMC solution. From the slopes of such linear plots, the exchange currents were calculated both for the anode and the cathode in the three different electrolytes and at different temperatures. Fig. 9 illustrates the Arrhenius plots for the anode kinetics in three different electrolytes. As may be seen from the figure, the slopes for the Arrhenius plots, or the activation energies for anode reaction, are nearly identical in the three electrolytes studied. For the cathode process, however, there is an interesting trend (Fig. 10). The cathode kinetics in the high EC-content solution were quite favorable at 25 °C, but become more sluggish at low temperatures, compared to the low-EC formulations. This "cross-over" in behavior occurs around −20 °C. A similar trend was also observed in the cell performance, which suggests that it may now be understood in terms of changes in the cathode kinetics.

3.1.4. Tafel polarization

The Tafel measurements were performed once again at slow enough scan rates to allow near-steady state conditions, but rapid enough not to cause significant changes in the state of charge for the materials during these measurements. Fig. 11 shows the typical Tafel curves of the cathode in one electrolyte, i.e., 1.0 M $LiPF_6$ in EC:EMC (20:80, v/v%). At room temperature not shown in figure, there is evidence of strong mass transfer interfer-

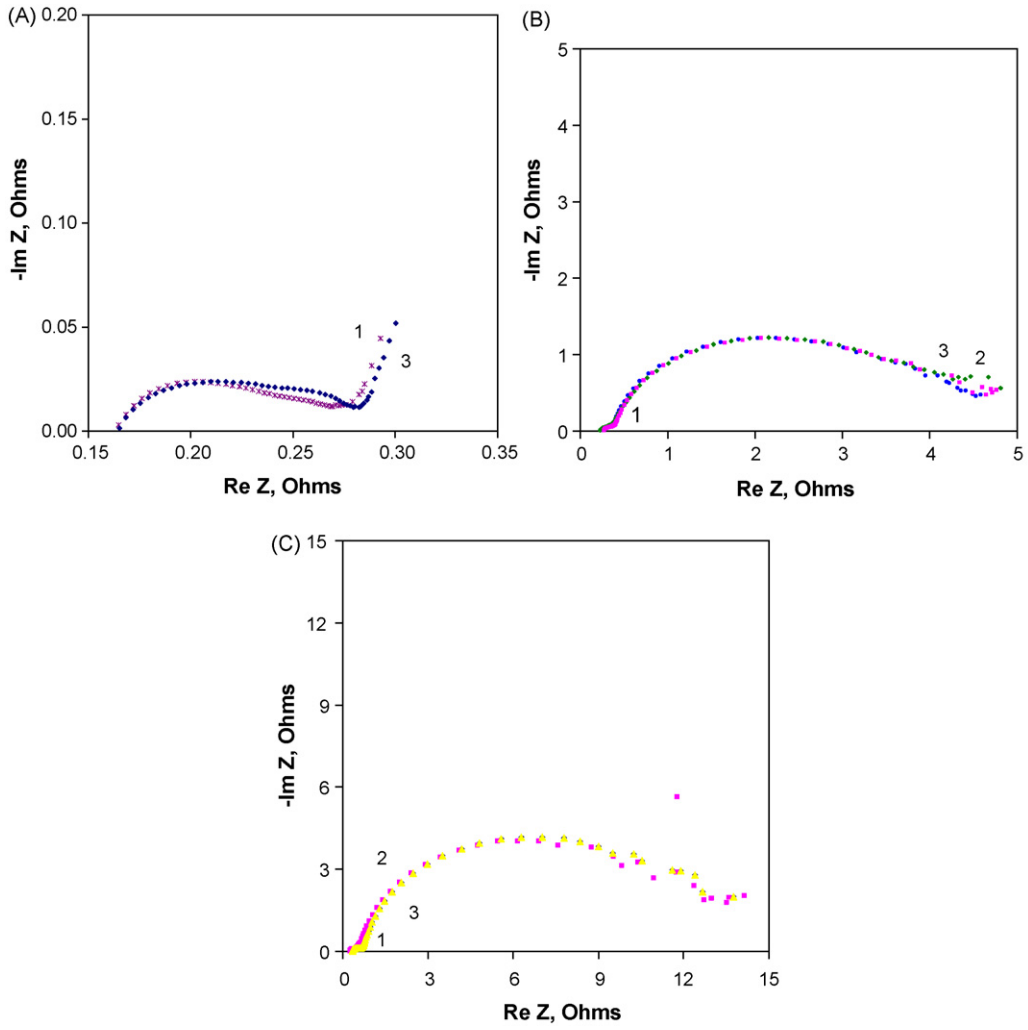

Fig. 6. EIS plots of graphite anode in (1) 1.0 M $LiPF_6$/EC:EMC (20:80), (2) 1.2 M $LiPF_6$/EC:EMC (20:80) and (3) 1.2 M $LiPF_6$/EC:EMC (30:70) electrolyte solutions at (A) 25 °C, (B) −20 °C and (C) −30 °C, respectively.

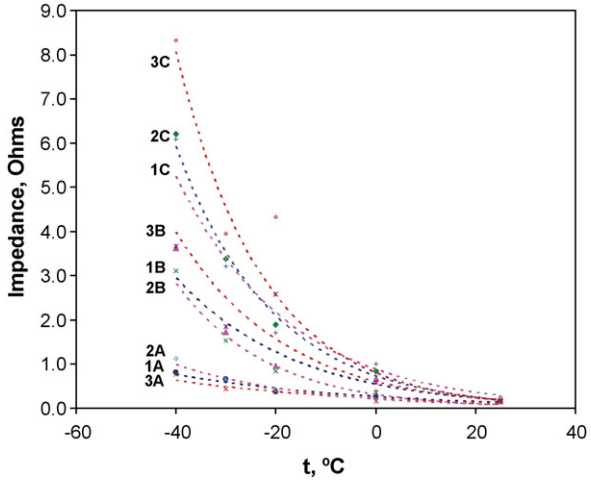

Fig. 7. Impedance from EIS measurements of $LiNi_{1/3}Mn_{1/3}Co_{1/3}O_2$ cathode in (1) 1.0 M $LiPF_6$/EC:EMC (20:80), (2) 1.2 M $LiPF_6$/EC:EMC (20:80) and (3) 1.2 M $LiPF_6$/EC:EMC (30:70) electrolyte solutions as a function of temperature at (A) 200 Hz, (B) 1 Hz and (C) 50 mHz, respectively.

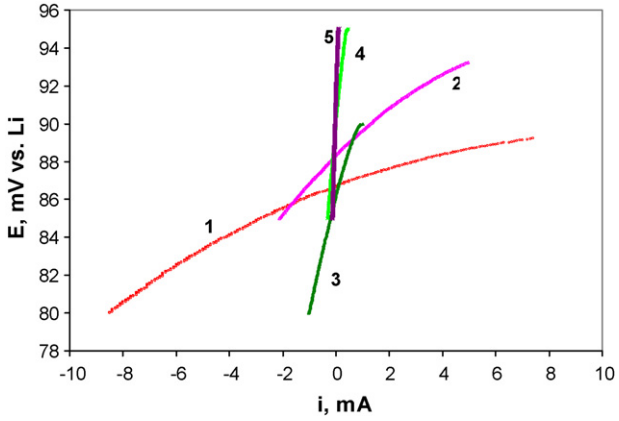

Fig. 8. dc linear polarization plots of graphite anode in 1.0 M $LiPF_6$/EC:EMC (20:80) electrolyte solution at: (1) 25 °C, (2) 0 °C, (3) −20 °C, (4) −30 °C and (5) −40 °C, respectively.

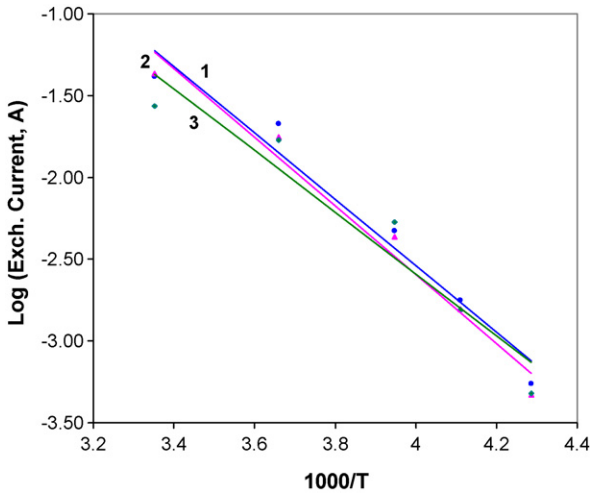

Fig. 9. Arrhenius plots from linear polarization for the Li intercalation in graphite in (1) 1.0 M $LiPF_6$/EC:EMC (20:80), (2) 1.2 M $LiPF_6$/EC:EMC (20:80) and (3) $LiPF_6$/EC:EMC (30:70) electrolyte solutions.

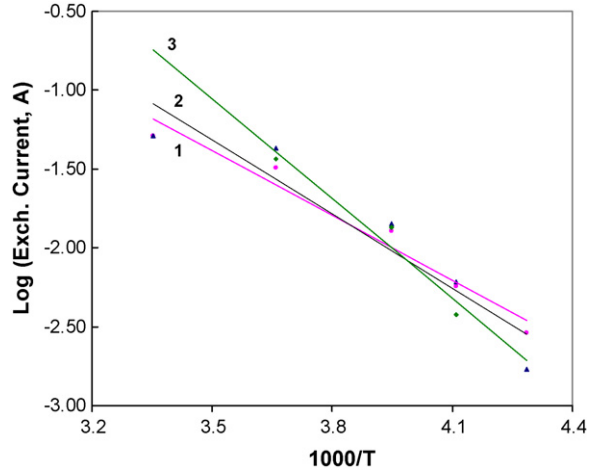

Fig. 10. Arrhenius plots from linear polarization for the charge transfer process on the $LiNi_{1/3}Mn_{1/3}Co_{1/3}O_2$ cathode in (1) 1.0 M $LiPF_6$/EC:EMC (20:80), (2) 1.2 M $LiPF_6$/EC:EMC (20:80) and (3) 1.2 M $LiPF_6$/EC:EMC (30:70) electrolyte solutions.

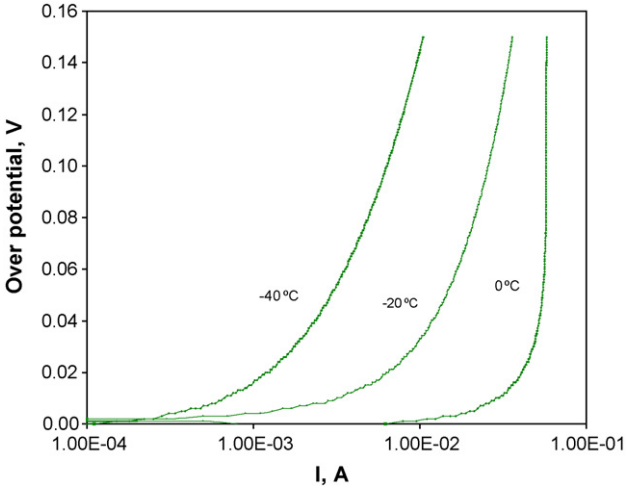

Fig. 11. Tafel polarization plots of $LiNi_{1/3}Mn_{1/3}Co_{1/3}O_2$ cathode in 1.0 M $LiPF_6$/EC:EMC (20:80) at different temperatures.

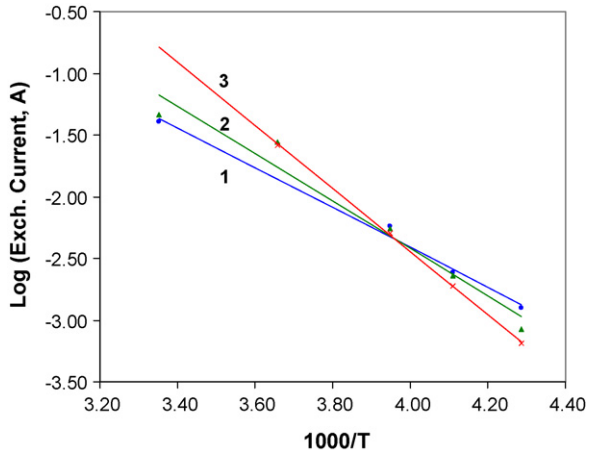

Fig. 12. Arrhenius plots from the Tafel polarization for the charge transfer process on the $LiNi_{1/3}Mn_{1/3}Co_{1/3}O_2$ cathode in (1) 1.0 M $LiPF_6$/EC:EMC (20:80), (2) 1.2 M $LiPF_6$/EC:EMC (20:80) and (3) $LiPF_6$/EC:EMC (30:70) electrolyte solutions.

ence at high discharge currents. At low temperatures, on the other hand, possibly due to a reduction in the charge transfer kinetics, the mass transfer influence is less significant. After applying corrections to the mass transfer effects, exchange currents were calculated from the revised Tafel plots. Figs. 12 and 13 illustrate the Arrhenius plots, based on these exchange currents for cathode and anode, respectively. Consistent with the observations from the dc linear polarization results, the cathode kinetics show a strong dependence on the electrolyte composition, with a crossover occurring around −20 °C. The anode kinetics, on the other hand, are slowed at low temperature to the same degree in all the three electrolytes. This finding is rather counter-intuitive from the current understanding that the electrolyte composition tends to affect the composition and morphology of the SEI on the carbon anode and thus impact Li intercalation/deintercalation at the anode/electrolyte interphase. Even though, such surface films (SEI) are reportedly possible on the cathode, their impact on the kinetics and hence on the cathode performance was believed to be not as overwhelming.

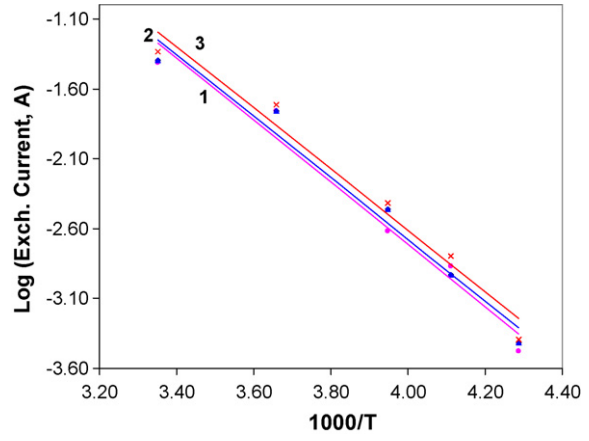

Fig. 13. Arrhenius plots from the Tafel polarization for the Li intercalation in graphite in (1) 1.0 M $LiPF_6$/EC:EMC (20:80), (2) 1.2 M $LiPF_6$/EC:EMC (20:80) and (3) 1.2 M $LiPF_6$/EC:EMC (30:70) electrolyte solutions.

4. Conclusions

The lithiated nickel manganese cobalt oxide $Li_{1+x}(Co_{1/3}Ni_{1/3}Mn_{1/3})_{1-x}O_2$, also termed as NMC cathode shows good compatibility with the carbonate-based low-temperature electrolytes. Impressive performances have been realized at low temperatures of $\leq -30\,^{\circ}C$. Electrolytes containing high salt concentration and high EC-content fare well at room temperatures. At low temperatures, on the other hand, the formulations with low EC-content and low salt concentration are preferred. Consistent with the electrical performance, the electrochemical kinetics of cathode in particular show a strong dependence on the nature of electrolytes at different temperatures, with a cross-over in from high EC solutions to low-EC formulations around $-20\,^{\circ}C$. The anode kinetics, on the other, decrease monotonously in the three electrolytes. The activation energies observed for the charge transfer processes at the cathode as well anode are consistent from the linear and Tafel polarization data. Further studies on the storage characteristics and high temperature resilience in these electrolytes are in progress.

Acknowledgements

The work described here was carried out at the Jet Propulsion Laboratory, California Institute of Technology, under contract with the National Aeronautics National Aeronautics and Space Administration (NASA), for the Exploration Systems Mission Directorate.

References

[1] M.C. Smart, B.V. Ratnakumar, L. Whitcanack, S. Surampudi, J. Byers, R. Marsh, IEEE Aerosp. Electr. Syst. Mag. 14 (11) (1999) 36–42.
[2] B.V. Ratnakumar, M.C. Smart, A. Kindler, H. Frank, R. Ewell, S. Surampudi, J. Power Sources 119-12 (2003) 906–910.
[3] M.C. Smart, B.V. Ratnakumar, L. Whitcanack, K. Chin, S. Surampudi, H. Croft, D. Tice, R. Staniewicz, J. Power Sources 119-12 (2003) 349–358.
[4] M.C. Smart, B.V. Ratnakumar, S. Surampudi, J. Electrochem. Soc. 149 (4) (2002) A361–A370.
[5] K. Amine, J. Liu, I. Belharouak, S.H. Kang, I. Bloom, D. Vissers, G. Henriksen, J. Power Sources 146 (1/2) (2005) 111–115.
[6] I. Belharouak, Y.I.K. Sun, J. Liu, K. Amine, J. Power Sources 123 (2) (2003) 247–252.
[7] M. Yoshio, H. Noguchi, J. Itoh, M. Okada, T. Mouri, J. Power Sources 90 (2000) 176.
[8] K.M. Shaju, G.V.S. Rao, B.V.R. Chowdari, Electrochim. Acta 48 (2002) 145.
[9] N. Yabuuchi, T. Ohzuku, J. Power Sources 119–121 (2003) 171.
[10] J. Choi, A. Manthiram, J. Electrochem. Soc. 152 (9) (2005) A1714–A1718.
[11] J. Barthel, H.-J. Gores, Pure Appl. Chem. 57 (8) (1985) 1071–1082.